

Mono- and dual-frequency fast cerebellar oscillation in mice lacking parvalbumin and/or calbindin D-28k

L. Servais,^{1,2} B. Bearzatto,² B. Schwaller,³ M. Dumont,⁴ C. De Saedeleer,⁵ B. Dan,⁵ J. J. Barski,⁶ S. N. Schiffmann² and G. Cheron^{1,5}

¹Laboratoire d'électrophysiologie, Université de Mons Hainaut, 24 Avenue du Champ de Mars, 7000 Mons, Belgium

²Laboratory of Neurophysiology CP601, Free University of Brussels, Brussels, Belgium

³Division of Histology, Department of Medicine, University of Fribourg, Fribourg, Switzerland

⁴Department of Biological Physics, University of Mons-Hainaut, Mons, Belgium

⁵Laboratory of Movement Neurophysiology and Biomechanics, Free University of Brussels, Brussels, Belgium

⁶Institute of Physiology, Ludwig-Maximilians University Munich, Munich, Germany

Keywords: Ca²⁺-binding proteins, cerebellum, complex spike, rhythmicity, simple spike, synchronicity

Abstract

Calbindin is a fast Ca²⁺-binding protein expressed by Purkinje cells and involved in their firing regulation. Its deletion produced ~160-Hz oscillation sustained by synchronous, rhythmic Purkinje cells in the cerebellar cortex of mice. Parvalbumin is a slow-onset Ca²⁺-binding protein expressed in Purkinje cells and interneurons. In order to assess its function in Purkinje cell firing regulation, we studied the firing behavior of Purkinje cells in alert mice lacking parvalbumin (PV^{-/-}), calbindin (CB^{-/-}) or both (PV^{-/-}CB^{-/-}) and in wild-type controls. The absence of either protein resulted in Purkinje cell firing alterations (decreased complex spike duration and pause, increased simple spike firing rate) that were more pronounced in CB^{-/-} than in PV^{-/-} mice. Cumulative effects were found in complex spike alterations in PV^{-/-}CB^{-/-} mice. PV^{-/-} and CB^{-/-} mice manifested ~160-Hz oscillation that was sustained by Purkinje cells firing rhythmically and synchronously along the parallel fiber axis. This oscillation was dependent on GABA_A, N-methyl-D-aspartate and gap junction transmission. PV^{-/-}CB^{-/-} mice exhibited a dual-frequency (110 and 240 Hz) oscillation. The instantaneous spectral densities of both components were inversely correlated. Simple and complex spikes of Purkinje cells were phase-locked to one of the two oscillation frequencies. Mono- and dual-frequency oscillations presented similar pharmacological properties. These results demonstrate that the absence of the Ca²⁺ buffers parvalbumin and calbindin disrupts the regulation of Purkinje cell firing rate and rhythmicity *in vivo* and suggest that precise Ca²⁺ transient control is required to maintain the normal spontaneous arrhythmic and asynchronous firing pattern of the Purkinje cells.

Introduction

Calbindin D-28k (CB) and parvalbumin (PV) are two Ca²⁺-binding proteins involved in intracellular Ca²⁺ homeostasis in conjunction with many other mechanisms (Fierro *et al.*, 1998). Both proteins are expressed in mostly non-overlapping neuron subpopulations (Celio, 1990; for a review, see Andressen *et al.*, 1993). Cerebellar Purkinje cells represent one of the few exceptions, as they highly express both proteins (for a review, see Schwaller *et al.*, 2002). CB and PV play different roles in the [Ca²⁺]_i regulation of Purkinje cells as CB is a fast buffer, whereas PV acts as a slow-onset buffer (Lee *et al.*, 2000; Schmidt *et al.*, 2003). In the cerebellum, CB is exclusively expressed in Purkinje cells (Celio, 1990), whereas PV is additionally expressed in inhibitory basket and stellate cells (Fortin *et al.*, 1998). Granule, Lugaro and unipolar brush cells do not express PV and CB but another fast calcium-binding protein, calretinin (CR). This latter is known to tightly regulate granule cell excitability (Gall *et al.*, 2003).

To investigate the functions of these proteins, mice deficient for CB (CB^{-/-}), PV (PV^{-/-}) or both (PV^{-/-}CB^{-/-}) have been generated (Airaksinen *et al.*, 1997; Schwaller *et al.*, 1999; Vecellio *et al.*, 2000).

Spatiotemporal aspects of Ca²⁺ transients in Purkinje cells of these mice confirmed the differential effect of CB and PV at the cellular level. Indeed, absence of the rapid buffer CB results in an increased amplitude of Ca²⁺ transients and a faster rate of [Ca²⁺]_i decay following climbing fiber stimulation (Airaksinen *et al.*, 1997; Barski *et al.*, 2003). In contrast, the slow-onset buffer PV does not affect the initial amplitude of Ca²⁺ transients but accelerates the initial decay of [Ca²⁺]_i in dendrites of Purkinje cells after parallel fiber stimulation (Schmidt *et al.*, 2003). Whether or not these differences in Ca²⁺-binding properties and localization result in different alterations of Purkinje cells firing *in vivo* remains unknown. *In vivo*, the cerebellum of CB^{-/-} mice manifests a 160-Hz local field potential oscillation (LFPO) supported by the synchronous rhythmic firing pattern of Purkinje cells along the parallel fiber axis supported by the synchronous rhythmic firing pattern of Purkinje cells (Cheron *et al.*, 2004). This LFPO further phase-locks Purkinje cells along the parallel fiber axis (Servais & Cheron, 2005). It is not known if this very fast oscillation of the local field is related to specific Ca²⁺-binding properties of CB or if fast cerebellar oscillation constitutes a pathophysiological, or compensatory, state common to different cerebellar network perturbations leading to an increased intrinsic or extrinsic excitation of the Purkinje cells. Indeed, mice lacking CR, another fast Ca²⁺ buffer almost exclusively expressed by granule cells

Correspondence: Dr L. Servais, ¹Laboratoire d'électrophysiologie, as above.
E-mail: servais.laurent@ulb.ac.be; gcheron@ulb.ac.be

Received 11 March 2005, revised 31 May 2005, accepted 5 June 2005

in the cerebellum, display a similar fast cerebellar oscillation sustained by the synchronization of rhythmic Purkinje cells along the parallel fiber axis (Cheron *et al.*, 2004). In this context, *in vivo* cerebellar electrophysiology in PV^{-/-} and PV^{-/-}CB^{-/-} mice offers new opportunities to assess the functional effects of these specific deletions on the output signals of the cerebellar cortex.

Materials and methods

Animal maintenance and genotyping

PV^{-/-} and CB^{-/-} mice, both generated on a mixed C57BL/6J × 129 genetic background [ES cell lines R1 (Airaksinen *et al.*, 1997) and E14 (Schwaller *et al.*, 1999)], were used to breed double knockout mice (PV^{-/-}CB^{-/-}) (Vecellio *et al.*, 2000). For some experiments, PV^{-/-} mice backcrossed to C57BL/6J for eight generations were used and called C57 PV^{-/-}. All animals were genotyped by polymerase chain reaction. The experimenters were blinded to the genotype in all experiments. Animals were kept in accordance with the international guidelines for the care and use of laboratory animals and the study was approved by the ethical committee of the University of Mons-Hainaut.

Histochemistry

Mice were decapitated under light ether anesthesia. The brain was removed and fixed for 24 h in 0.1 M phosphate-buffered 4% paraformaldehyde freshly prepared at 4 °C. Following a wash in 0.1 M phosphate-buffered saline and consecutive 24-h incubations in 10, 20 and 30% sucrose solutions, brains were embedded in Tissue-Tek OCT compound (Miles, Elkhart, IN, USA), frozen in 2-methyl butane, cooled on dry ice and stored at -80 °C. Cryostat-cut 30-µm-thick brain parasagittal sections were processed free-floating. After quenching of the endogenous peroxidases, the floating sections were incubated for 1 h in 10% swine normal serum (Hormonology Laboratory, Marloie, Belgium). Sections were then incubated overnight at room temperature (21 °C) with anti-CR polyclonal antiserum (1 : 1000, Swant, Bellinzona, Switzerland). Thereafter, they were successively incubated with swine anti-rabbit gamma globulins (1 : 30, DAKO, Glostrup, Denmark) and rabbit peroxidase anti-peroxidase (PAP) complex (1 : 300, DAKO). The peroxidase activity was revealed by diaminobenzidine in the presence of hydrogen peroxide.

In vivo electrophysiology

Surgical preparation for recording

Under general anesthesia with xylido-dihydrothiazin (Rompun[®], Bayer, 10 mg/kg) and ketamine (Ketalar[®], Pfizer, 100 mg/kg), 31 mice with a mixed C57BL/6J × 129 background [nine PV^{-/-}, four PV^{-/-}CB^{-/-}, nine CB^{-/-} and nine wild-type (WT)] and six C57 PV^{-/-} mice aged 10–13 months (24–35 g) were prepared for chronic extracellular recording of neuronal activity in the cerebellum (Cheron *et al.*, 2004). Anesthesia was monitored clinically and a supplement dose of xylido-dihydrothiazin (3 mg/kg) and ketamine (30 mg/kg) was administered if the animal presented agitation or markedly increased respiration or heart rate during the procedure. In addition, local anesthesia with 0.5 mL Lidocaine (20 mg/mL) plus Epinephrine (1 : 80 000) (Xylocaine[®], Astra Zeneca) was administered subcutaneously during soft tissue removal. The two different backgrounds of PV^{-/-} mice were used in this study in order to exclude the possibility that the observed properties were dependent on the genetic back-

ground. As no differences were found in any of the studied parameters between PV^{-/-} strains with the two different genetic backgrounds, data from all the PV^{-/-} mice were pooled.

Two small bolts were cemented to the skull to immobilize the head during the experimental session. The surface of the uvula of the cerebellum was exposed by reflecting the muscles overlying the cisterna magna, a craniotomy was performed above the cerebellum and an acrylic recording chamber constructed around the craniotomy. Mice were allowed to recover from anesthesia for 24 h. The dura mater was removed locally above the vermis just prior to the recording session.

Single unit recording and analysis

Single unit recordings were performed with glass micropipettes (1.5–5 MΩ impedance). A signal was considered as originating from a Purkinje cell if it presented two types of spiking activities: simple spikes, characterized by single depolarization (300–800 µs) occurring at high frequencies (~50 Hz), and less frequent complex spikes (0.5–1 Hz), characterized by an initial fast depolarization (300–600 µs) followed by smaller components in a relatively consistent manner for the same Purkinje cell. Simple and complex spikes were considered to originate from the same Purkinje cell if a transient pause in simple spike firing followed each complex spike. The duration of the complex spike was defined as the time between the first and last depolarization. Depolarizations were counted as long as their amplitude reached at least twice the maximum amplitude of the background signal. Pause duration was measured as the period between the first depolarization of the complex spike and the first following simple spike in a cross-correlogram of simple spike firing triggered by complex spikes. After amplification (by a factor of 1000–2000) and band-pass filtering (10 Hz–10 kHz), unit activity was continuously stored on 4-mm digital audio tapes, transferred to a Pentium III personal computer with analog-to-digital converter boards (Power 1401, CED) and analysed off-line with Spike 2 CED software. The recorded data were digitized continuously at 10 kHz.

For each Purkinje cell recording lasting more than 2 min, the simple spike autocorrelogram was constructed using time bins of 1 ms. The rhythmic frequency was defined as the reciprocal of the latency of the first peak in the autocorrelogram. The strength of the rhythmicity was quantified with a rhythm index (Sugihara *et al.*, 1995). Consequently, the rhythmicity of each cell was quantified according to its strength and frequency.

Multi-unit recording

Multiple recordings along the same parallel fiber axis were recorded by means of seven linearly arranged, quartz-insulated, platinum-tungsten fiber microelectrodes (outer and shaft diameter, 80 and 25 µm, respectively) with 250-µm interelectrode spacing. Each microelectrode was mounted into a stretched elastic rubber tube allowing individual control of tip position by means of DC micromotors (resolution, 0.27 µm) (Eckhorn & Thomas, 1993).

Local field potential analysis

Local field potentials were analysed by the wave-triggered averaging technique (Steriade *et al.*, 1998). Negative peaks of the LFPO were taken as the starting point and symmetrical time windows (50 ms before and 50 ms after) were extracted and averaged. These averaged oscillation sequences were quantified by a Fast-Fourier-Transform algorithm. An oscillation index was computed by dividing the maximum amplitude of the power spectrum peak by the total area of the power spectrum (Cheron *et al.*, 2004).

In order to test the spatial coherence of LFPO along the coronal plane (i.e. along the same parallel fiber beam), cross-correlation functions between each set of two LFPOs (α_1, α_2) were calculated. The span of time lags or leads was analysed for a time window (T) corresponding to a recording period of 0.6 s. The cross-correlation function between two functions, e.g. α_1 and α_2 , was defined as:

$$CCF_{\alpha_1, \alpha_2}(\tau) = \frac{1}{T\sigma_1\sigma_2} \int_0^T (\alpha_1(t) - \mu_1)(\alpha_2(t + \tau) - \mu_2) dt$$

where μ_i and σ_i are the mean value and the variance of α_i and τ is the lag between the two functions. When the signals $\alpha_1(t)$ and $\alpha_2(t)$ are statistically correlated, their cross-correlation function displays a peak (a significant cross-correlation function maximum) or a trough (a significant cross-correlation function minimum) at the abscissa τ^* . Positive values of τ^* denote a time lead of $\alpha_1(t)$ relative to $\alpha_2(t)$, whereas negative values denote a time lag.

In case of dual-frequency components in the LFPO, the recorded data were treated using the finite impulse response method, band-pass filters (70 dB/octave) centred around one of the two Fast-Fourier-Transform peaks (the band range extended from 10 Hz above and below the central peak). These filtered data were then separately analysed with a 512-point window Fast-Fourier-Transform since the first point of the recording. The square of the spectral density of both dominant frequencies was calculated in the corresponding window and the window was then displaced along the recording (step of 5 ms) so that the spectral density of each frequency could be plotted relative to time. A cross-correlation function similar to that described above was adopted in order to decipher the temporal relationship between the two frequency components of the dual-frequency LFPO recorded in $PV^{-/-}CB^{-/-}$ mice. In this case α_1, α_2 corresponded to the square of the spectral density of the two basic rhythms.

Drug microinjection

Injection micropipettes, drawn from calibrated 1.16-mm internal diameter glass tubing (internal diameter, 30 μ m), were filled with either a solution of 27 mM SR95531 (GABA_A antagonist) (Sanofi, Paris, France), 6 mM APV (*N*-methyl-D-aspartate antagonist) (Sigma) or 48 mM carbenoxolone (gap junction blocker) (Sigma). All substances were used as a solution in saline. Injections (10 pulses of 10-ms duration) were carried out using an air pressure system (Picospritzer II).

Statistical analysis

Data were analysed using a one-way ANOVA test and Bonferroni's post-hoc test after assessing their normality by a Kolmogorov-Smirnov test. Differences were considered significant at $P < 0.05$. Results are expressed as mean \pm 1 SD.

Results

Firing behavior of individual Purkinje cells in vivo

We compared Purkinje cells firing in the different mutant groups with WT controls. Signals were recorded from a total of 281 Purkinje cells (67 in WT, 78 in $PV^{-/-}$, 77 in $CB^{-/-}$ and 59 in $PV^{-/-}CB^{-/-}$ mice). A typical recording is shown in Fig. 1A. Simple spike firing rates of Purkinje cells were significantly increased in $PV^{-/-}$, $CB^{-/-}$ and $PV^{-/-}CB^{-/-}$ in comparison with WT mice ($P < 0.0001$, one-way ANOVA) but no significant differences existed between the groups of

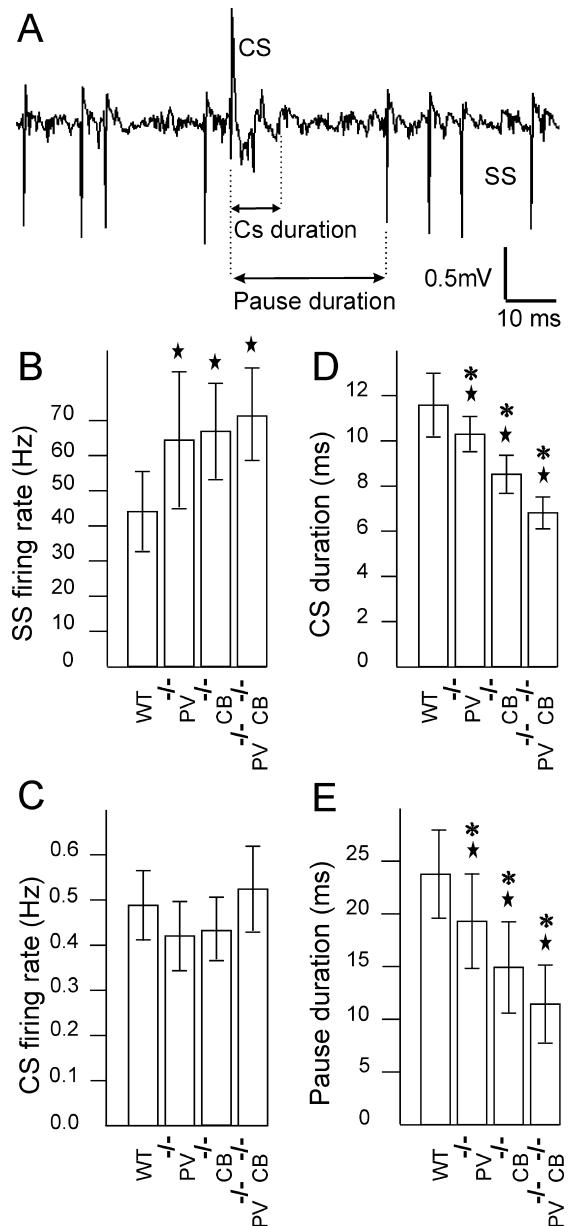


FIG. 1. (A) Typical extracellular recording of a Purkinje cell in an alert wild-type (WT) mouse. The complex spike (CS) is easily discriminated from the simple spike (SS). (B) SS firing rate in Purkinje cell of WT and mice lacking parvalbumin ($PV^{-/-}$), calbindin ($CB^{-/-}$) and calbindin and parvalbumin ($PV^{-/-}CB^{-/-}$). (C) CS firing rate in Purkinje cell of WT, $PV^{-/-}$, $CB^{-/-}$ and $PV^{-/-}CB^{-/-}$ mice. There is no significant difference between groups. (D) CS duration in the same Purkinje cells. (E) Pause duration in the same Purkinje cells. Stars and asterisks indicate significant differences compared with WT and other mutant groups, respectively.

genetically modified mice (Fig. 1B). In contrast, the complex spike firing rates were not significantly different between WT, $PV^{-/-}$, $CB^{-/-}$ and $PV^{-/-}CB^{-/-}$ mice (Fig. 1C) ($P > 0.1$ one-way ANOVA). However, the duration of the complex spike was significantly longer in WT mice than in all mutants, the order being $PV^{-/-} > CB^{-/-} > PV^{-/-}CB^{-/-}$ (Fig. 1D) ($P < 0.0001$, one-way ANOVA). A similar ranking with respect to pause duration after complex spike firing was observed in the three transgenic strains ($P < 0.0001$, one-way ANOVA). In comparison with WT, the pause duration decreased in $PV^{-/-}$, even more in $CB^{-/-}$ and even more in $PV^{-/-}CB^{-/-}$ mice (Fig. 1E). Again significant differences existed between all groups.

Emergence of spontaneous mono and dual oscillations

The most remarkable electrophysiological feature of the cerebellum of $PV^{-/-}$, $CB^{-/-}$ and $PV^{-/-}CB^{-/-}$ mice was the presence of a spontaneous LFPO about 160–200 Hz (Fig. 2A and B) during ~50% of the recording time. Episodes of spontaneous LFPO were found throughout the explored cerebellar regions (vermis, uvula and nodulus) of $PV^{-/-}$, $CB^{-/-}$ and $PV^{-/-}CB^{-/-}$ mice. They appeared as episodes of spindle-shaped oscillation with a mean rate of occurrence of 4.3 ± 1.5 spindle/s. Oscillations with an oscillation index > 5 were recorded in 12 out of the 15 $PV^{-/-}$, in all four $PV^{-/-}CB^{-/-}$, in all nine $CB^{-/-}$ and in none of the WT mice. The oscillation index was not significantly different between mutant mice (12.2 ± 4.3 , 9.9 ± 5.5 and 10.4 ± 3.4 in $CB^{-/-}$, $PV^{-/-}$ and $PV^{-/-}CB^{-/-}$ mice, respectively) ($P > 0.2$, one-way ANOVA). The frequency of oscillation was not significantly different between $CB^{-/-}$ and $PV^{-/-}$ mice ($P > 0.6$, one-way ANOVA) (Fig. 2C). In contrast to mice deficient for either one of the Ca^{2+} -binding proteins, LFPO in $PV^{-/-}CB^{-/-}$ mice showed two frequency peaks during approximately 50% of the oscillation recording time (Fig. 2D and E). The difference between the two oscillation frequencies was always larger than 100 Hz (Fig. 2F). During the same recording session, the dual-frequency oscillation could progressively

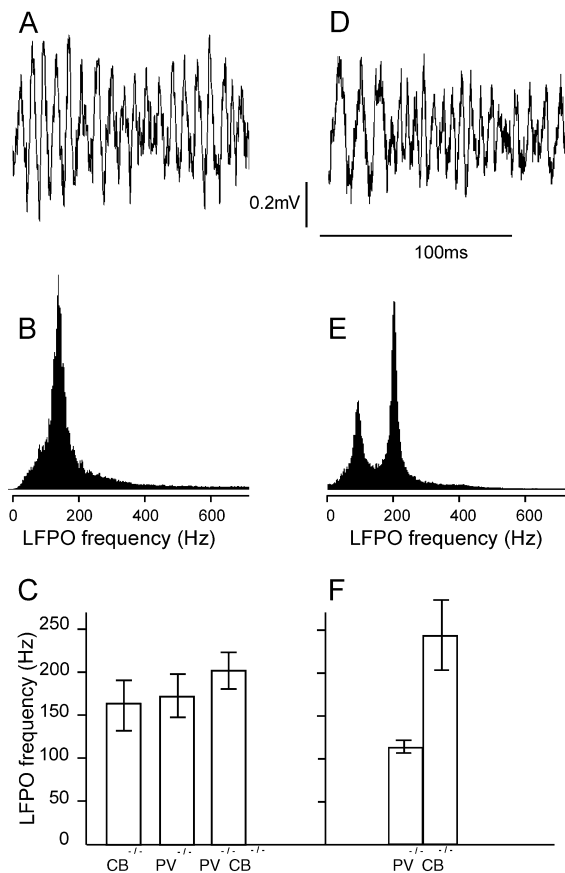


FIG. 2. Mice lacking parvalbumin ($PV^{-/-}$), calbindin ($CB^{-/-}$) or both ($PV^{-/-}CB^{-/-}$) present fast cerebellar oscillations. (A) Local field potential oscillation (LFPO) recorded in the most superficial layer of the cerebellum of a $PV^{-/-}$ mouse. (B) Fourier spectrum of the LFPO illustrated in A computed from a 60-s oscillation period. (C) Frequency of LFPO episodes recorded in nine $CB^{-/-}$, 12 $PV^{-/-}$ and two $PV^{-/-}CB^{-/-}$ mice that presented episodes of mono-frequency oscillations ($n = 8$ episodes). Dual-frequency LFPO recorded in a $PV^{-/-}CB^{-/-}$ mouse (D) and the corresponding Fourier spectrum (E). (F) Frequency of oscillations recorded in four $PV^{-/-}CB^{-/-}$ mice that manifested dual-frequency oscillations ($n = 12$ episodes).

switch to a mono-frequency oscillation with an intermediate frequency of 201.0 ± 21 Hz (Fig. 2E), which was significantly different from the frequencies observed in single knockout mice ($P < 0.05$, one-way ANOVA).

Given the presence of fast LFPO in the cerebellum of mutant mice lacking Ca^{2+} -binding proteins of different properties and cellular localization, we examined whether the electrophysiological and pharmacological properties of these oscillations were similar.

Spatiotemporal mapping of the oscillation

As the LFPO of $CB^{-/-}$ mice is highly synchronized along the parallel fiber axis (Cheron *et al.*, 2004), we verified whether LFPO in $PV^{-/-}$ and $PV^{-/-}CB^{-/-}$ mice was spatiotemporally organized in the same way by measuring their cross-correlation function. Simultaneous recordings of mono-frequency LFPO in both groups showed a high degree of synchronization along the parallel fiber axis (Fig. 3). For all LFPO pairs separated by 250 μ m, the cross-correlation function reached a mean value of 0.68 ± 0.07 ($n = 5$) at a mean lag value close to zero (0.1 ± 0.1 ms) showing tight phase-locking of LFPO along the parallel fiber axis. With increasing distances (500, 750 μ m; $n = 5$) between the electrode pairs, the mean cross-correlation function values significantly decreased (0.40 ± 0.03 and 0.14 ± 0.04 , respectively) but lag values remained very close to zero (0.2 ± 0.1 and -0.1 ± 0.2 ms, respectively).

Pharmacological properties of local field potential oscillations

Local field potential oscillation in $CB^{-/-}$ mice is mediated by gap junctions, *N*-methyl-D-aspartate receptors and GABA_A receptors as LFPO in these mice is largely reduced by microinjection of carboxolone, APV and gabazine, respectively (Cheron *et al.*, 2004). Thus, we tested whether LFPOs in $PV^{-/-}$ and $PV^{-/-}CB^{-/-}$ mice have the same pharmacological properties as those described in $CB^{-/-}$ mice. To better assess the specificity of the three substances, we used only half-doses of those used in our previous study (Cheron *et al.*, 2004). As no significant differences in the responses to carboxolone, APV or gabazine were observed between $PV^{-/-}$ and $PV^{-/-}CB^{-/-}$ mice, data were pooled. Microinjections of carboxolone ($n = 13$) (Fig. 4A), APV (Fig. 4B) ($n = 8$) and gabazine (Fig. 4C) ($n = 5$) produced a significant reduction of the LFPO index after 1 min ($P < 0.05$, one-way ANOVA for repeated measures). These effects were reversible and values recovered to pre-injection values within 10 min (carboxolone), 4 min (APV) and 5 min (gabazine). If the substances were applied during dual-frequency oscillations in $PV^{-/-}CB^{-/-}$ mice, both frequency peaks were equally decreased.

Interaction between frequencies of dual-frequency oscillation

In order to better understand the interaction between the two frequencies of dual-frequency LFPO episodes in $PV^{-/-}CB^{-/-}$ mice, we studied the relationship between instantaneous spectral densities of both frequency peaks on eight episodes of dual-frequency LFPO recorded in four $PV^{-/-}CB^{-/-}$ mice. Raw LFPO episodes were recorded during 60 s (Fig. 5A) and a random sample of 0.8 s was then band-pass filtered 10 Hz above and below each frequency peak (Fig. 5B and C) and the filtered signals were quantified separately by measuring the instantaneous spectral density of their maximal frequency content (Fig. 5D). Cross-correlation analysis of the temporal relationship between these two instantaneous spectral density curves demonstrated that the two oscillating components were

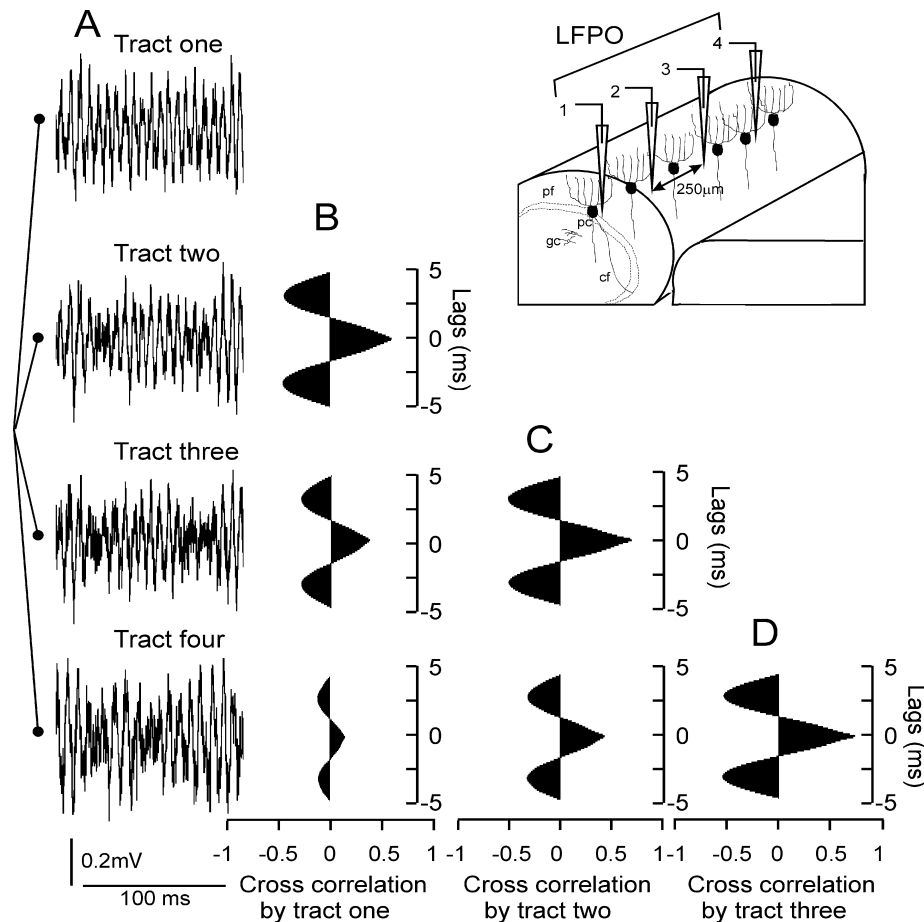


FIG. 3. Fast cerebellar oscillation is synchronized along the parallel fiber beam. (A) Simultaneous recording of four local field potential oscillation (LFPO) episodes recorded at the surface of the cerebellar cortex in a mouse lacking parvalbumin (left). Electrodes are 250 μm apart and placed close to the Purkinje cell layer, along the parallel fiber beam (right). (B) Cross-correlation of tracts two, three and four with tract one. Note the decrement of the maximum cross-correlation amplitude as a function of the distance between the tracts. (C) Cross-correlation of tracts three and four with tract two. (D) Cross-correlation of tract three with tract four. CF, climbing fiber; GC, granule cell; PC, purkinje cell; PF, parallel fiber.

inversely correlated (maximum of cross-correlation function, -0.44 ± 0.08 ; time lag, 11.9 ± 36.8 ms) indicating the existence of two alternating rhythms (Fig. 5E).

Purkinje cell firing and mono-frequency local field potential oscillation

In order to further understand the relationship between Purkinje cell firing and LFPO, we compared Purkinje cells recorded during and in the absence of LFPO. In all mutants, simple spike frequency was much higher for Purkinje cells recorded during episodes of LFPO (110 ± 38 vs. 57 ± 22 Hz in $\text{CB}^{-/-}$, 112 ± 45 vs. 56 ± 15 Hz in $\text{PV}^{-/-}$ and 99 ± 59 vs. 62 ± 25 Hz in $\text{PV}^{-/-}\text{CB}^{-/-}$ mice, $P < 0.0001$, one-way ANOVA). The rhythmicity of simple spike firing in mutants was also much higher during LFPO. Indeed, the rhythm index of Purkinje cells recorded in the absence of LFPO was only slightly increased in $\text{CB}^{-/-}$ (0.013 ± 0.003 , $n = 14$), $\text{PV}^{-/-}$ (0.016 ± 0.003 , $n = 8$) and $\text{PV}^{-/-}\text{CB}^{-/-}$ (0.014 ± 0.002 , $n = 12$) in comparison with WT animals (0.006 ± 0.001 , $n = 36$) ($P < 0.001$, one-way ANOVA). No significant difference was found between the different groups of mutant mice. In contrast, the rhythm index of Purkinje cells recorded during LFPO episodes was significantly increased in all mutants as compared with WT and was much higher in $\text{CB}^{-/-}$ (0.16 ± 0.04 , $n = 17$) and $\text{PV}^{-/-}\text{CB}^{-/-}$ (0.17 ± 0.03 ,

$n = 29$) than $\text{PV}^{-/-}$ (0.05 ± 0.02 , $n = 26$) mice ($P < 0.0001$, one-way ANOVA). To further investigate the relationship between Purkinje cell rhythmicity, firing rate and LFPO, we recorded rhythmic Purkinje cells simultaneously during mono-frequency oscillation episodes in $\text{PV}^{-/-}$ ($n = 15$) and $\text{PV}^{-/-}\text{CB}^{-/-}$ ($n = 11$) mice. In each Purkinje cell, the averaged signal triggered by the simple or complex spike demonstrated coherent mono-frequency oscillation before and after the spike. This indicates that both simple and complex spike firings of the Purkinje cells were phase-locked to the LFPO. The firing behavior of two simultaneously recorded Purkinje cells in conjunction with the simultaneously recorded LFPO in a $\text{PV}^{-/-}$ mouse is illustrated in Fig. 6A. Autocorrelation analysis indicates that both cells were rhythmic in their simple spike firing (Fig. 6B for cell 1) and cross-correlation indicates that they were synchronized (Fig. 6C). The averaging of LFPO triggered by the simple spikes of a single Purkinje cell shows the presence of coherent LFPO symmetrical to the trigger (Fig. 6D). This indicates that the simple spike firing of the Purkinje cell was phase-locked to the LFPO. The complex spike of each Purkinje cell induced a ~ 10 – 15 -ms pause in its own simple spike firing (Fig. 6E) but not in the simple spike firing of the other cell (Fig. 6F). The averaging of LFPO triggered by the complex spike of a single Purkinje cell also shows coherent LFPO (Fig. 6G) but, in this case, the complex spike depolarization occurs in the ascending wave of the LFPO.

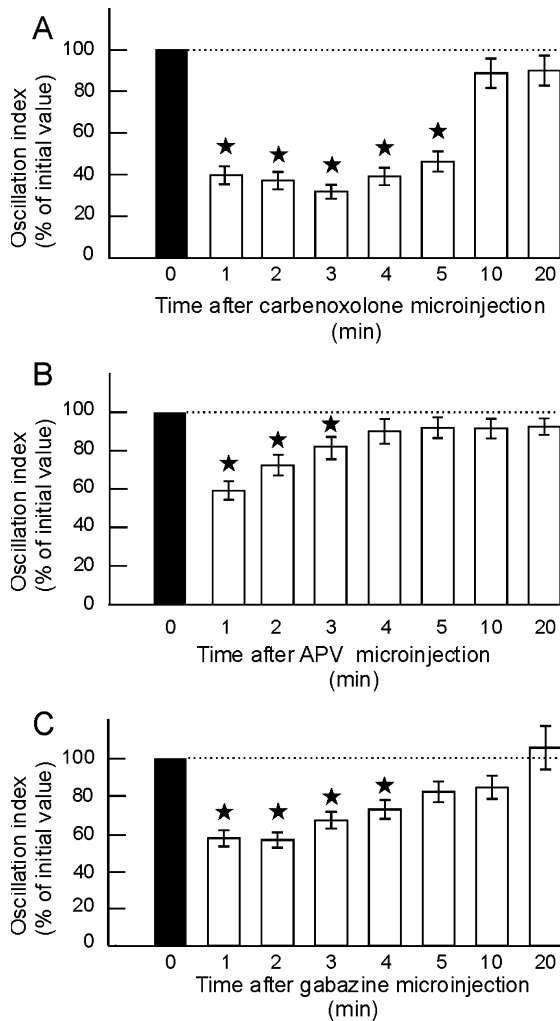


FIG. 4. Local field potential oscillation is diminished by the gap junction blocker carbenoxolone and by antagonist of the *N*-methyl-D-aspartate receptors (APV) and the GABA_A receptor inhibitor gabazine. (A–C) Oscillation index computed for a 60-s period either 1, 2, 3, 4, 5, 10 or 20 min after a cerebellar microinjection of carbenoxolone ($n = 13$), APV ($n = 8$) and gabazine ($n = 5$) in mice lacking parvalbumin and mice lacking calbindin and parvalbumin. The oscillation index is expressed as percent of initial value computed 60 s before the injection. Stars indicate significant differences compared with initial values.

Purkinje cell firing and dual-frequency local field potential oscillation

To assess whether the two frequencies of the dual-frequency LFPO are supported by different Purkinje cells, we simultaneously recorded rhythmic Purkinje cells and dual-frequency LFPO ($n = 7$). The firing behavior of a Purkinje cell during dual-frequency LFPO recorded in a $PV^{-/-}CB^{-/-}$ mouse is shown in Fig. 7A. The LFPO was band-pass filtered 10 Hz below and above the slow (Fig. 7B) and rapid (Fig. 7C) frequency peaks. Simple spike autocorrelation analysis indicates that the Purkinje cell was slightly rhythmic (Fig. 7D). The averaging of the raw LFPO triggered by the simple spikes shows coherent mono-frequency LFPO (Fig. 7E). In the illustrated case, the Purkinje cell was synchronized with the rapid frequency. The same procedure applied to the band-pass-filtered signal further confirmed the synchronization of the simple spike with the rapid frequency (Fig. 7F and G). As expected, the complex spike induced a ~15-ms pause in its own simple spike firing (Fig. 7H). Averaging of raw LFPO triggered by the complex

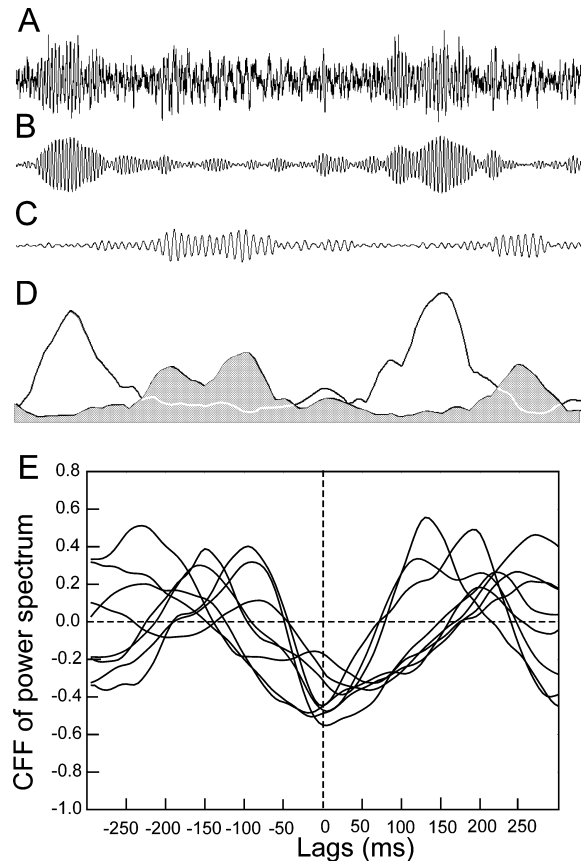


FIG. 5. The two frequencies of dual-frequency local field potential oscillation (LFPO) recorded in mice lacking calbindin and parvalbumin ($PV^{-/-}CB^{-/-}$) are inversely correlated. (A) LFPO recorded at a depth of 550 μ m from the vermis of a $PV^{-/-}CB^{-/-}$ mouse. (B) The same signal, band-pass filtered from 220 to 240 Hz. (C) The same signal as in A, band-pass filtered from 120 to 140 Hz. (D) Instantaneous spectral densities of band-pass-filtered signals illustrated in B (white) and C (gray). (E) Cross-correlation function (CCF) of instantaneous spectral densities in eight dual-frequency oscillations recorded in four $PV^{-/-}CB^{-/-}$ mice (duration 0.6 s).

spike also demonstrated coherent mono-frequency LFPO (Fig. 7I). This further confirms the synchronization of complex spikes with the rapid frequency. Synchronization was enhanced when averaging was performed on the band-pass-filtered signal (Fig. 7J and K). This type of analysis was performed on seven rhythmic Purkinje cells recorded during dual-frequency oscillations. As illustrated in Fig. 8A, the simple spike rhythmic frequency of Purkinje cells was phase-locked either to the slow (cells 5–7) or rapid (cells 1–4) frequency. This indicates that distinct populations of rhythmic Purkinje cells support one or other of the frequencies of the dual-frequency LFPO. The frequency of dual-frequency LFPO that was closest to the simple spike rhythmic frequency was chosen in further analyses.

Purkinje cell rhythmicity and oscillation frequency

With the aim of investigating a putative correlation between simple spike rhythmicity and LFPO, we analysed Purkinje cells recorded during LFPO periods in $PV^{-/-}$ ($n = 26$) and $PV^{-/-}CB^{-/-}$ mice ($n = 29$). Among the 29 Purkinje cells recorded in $PV^{-/-}CB^{-/-}$ mice, nine were recorded during dual-frequency LFPO. Of the 55 Purkinje cells, 33 presented an autocorrelation with multiple side peaks. These cells were recorded in $PV^{-/-}$ mice ($n = 15$), in $PV^{-/-}CB^{-/-}$ mice

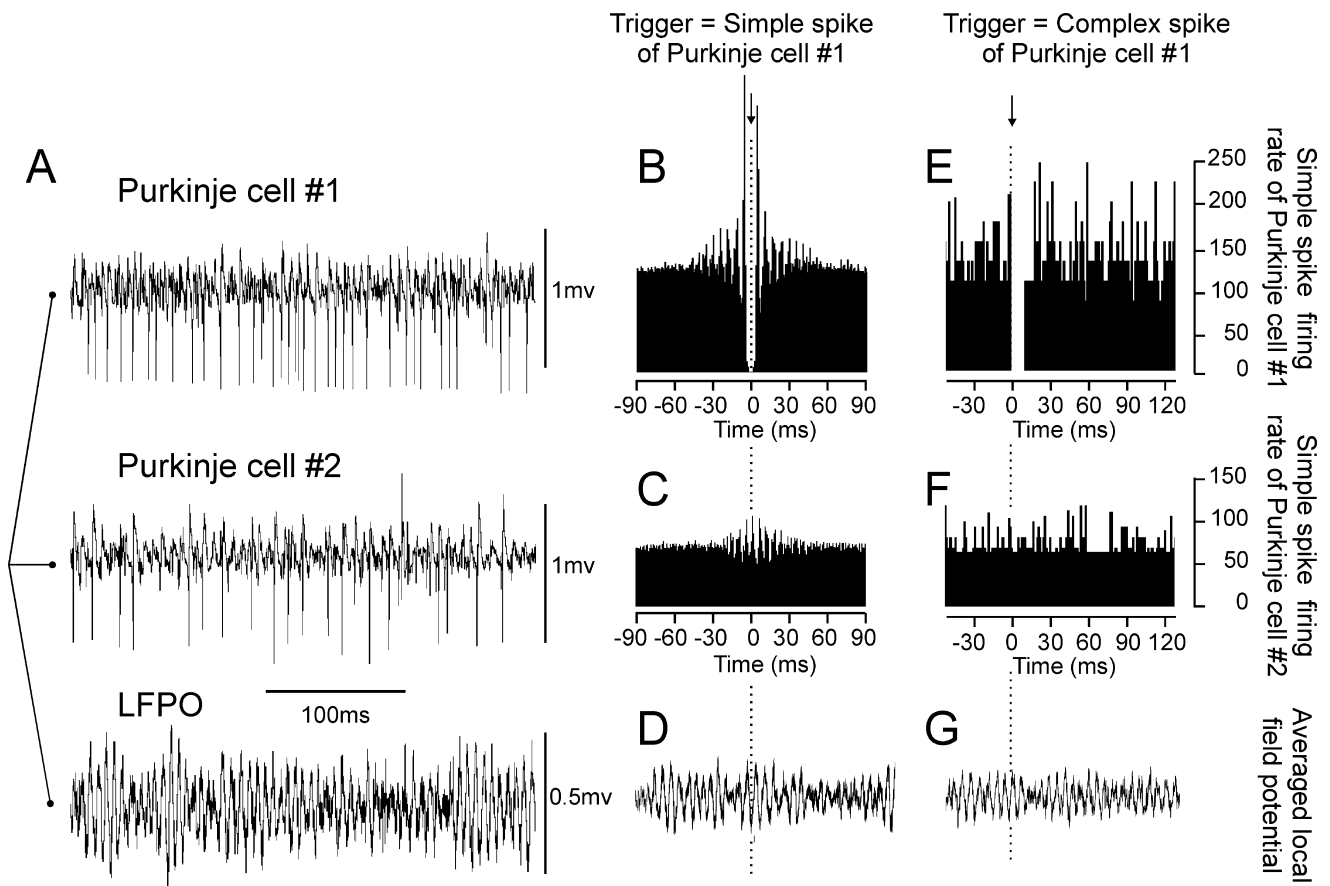


FIG. 6. Purkinje cells and local field potential oscillation (LFPO) are synchronized along the parallel fiber axis. (A) Simultaneous recording of two Purkinje cells and one LFPO by three electrodes spaced by 250 μm along the parallel fiber axis. (B) Simple spike autocorrelogram of Purkinje cell no. 1. (C) Simple spike cross-correlogram of Purkinje cell no. 2 triggered by simple spike of Purkinje cell no. 1. (D) Averaging of LFPO triggered by simple spike of Purkinje cell no. 1. Note that simple spike depolarization is phase-locked to the negative wave of the LFPO. (E) Simple spike cross-correlogram of Purkinje cell no. 1 triggered by the complex spike of Purkinje cell no. 1. Note the 10-ms pause in simple spike firing. (F) Simple spike cross-correlogram of Purkinje cell no. 2 triggered by the complex spike of Purkinje cell no. 1. Note that no pause in simple spike firing occurs. (G) Averaging of LFPO triggered by complex spike of Purkinje cell no. 1. Note that the depolarization of the complex spike is phase-locked to the ascending wave of the LFPO.

with mono-frequency LFPO ($n = 11$) and in $PV^{-/-}CB^{-/-}$ mice with dual-frequency oscillations ($n = 7$). We found a strong ($r = 0.88$) and significant ($P < 0.0001$) correlation between simple spike rhythmic frequency (Fig. 8B) and LFPO frequency.

Purkinje cells of $PV^{-/-}$ mice do not exhibit paradoxical immunoreactivity to anti-calretinin serum

The alterations in Purkinje cell firing behavior in $PV^{-/-}$ mice were similar to those previously described in CR-deficient mice ($CR^{-/-}$) (i.e. increase in simple spike frequency, decrease in complex spike and pause durations and emergence of 160-Hz oscillations) (Schiffmann *et al.*, 1999; Cheron *et al.*, 2004; Bearzatto *et al.*, 2004). This may suggest a possible common mechanism operating in both mutants. The positive staining of $CR^{-/-}$ Purkinje cells with an antiserum against CR was discussed as an increased fractional Ca^{2+} occupancy of CB leading to the cross-reactivity of the CR antibody to the Ca^{2+} -bound form of the closely related protein CB (Schiffmann *et al.*, 1999). The authors proposed that alterations in the Ca^{2+} homeostasis in Purkinje cells of $CR^{-/-}$ mice might be a likely explanation. As PV is also inferred to act in the regulation of Ca^{2+} homeostasis in Purkinje cells (Schmidt *et al.*, 2003), we tested whether the absence of PV leads to similar changes in the CR immunoreactivity of Purkinje cells. In WT

mice, CR immunoreactivity was confined to granule cells including the parallel fibers in the molecular layer, while Purkinje cells were completely negative (Fig. 9A and B). As demonstrated before, Purkinje cell somata, dendrites and axons were strongly labeled with the CR antiserum in $CR^{-/-}$ mice (Fig. 9C and D). In $PV^{-/-}$ as well as WT mice, however, CR staining in the cerebellum was confined to granule cells (Fig. 9E and F).

In the CB-deficient mice investigated here ($CB^{-/-}$ and $PV^{-/-}CB^{-/-}$ mice), no staining by the CR antiserum could be detected in Purkinje cells and CR immunoreactivity was confined to the granule cell layer and the parallel fibers in the molecular layer (similar to Fig. 9A and B, data not shown). This is in line with the fact that the apparent CR immunoreactivity in Purkinje cells of $CR^{-/-}$ mice is due to the presence of CB (Schiffmann *et al.*, 1999).

Discussion

This study demonstrates Purkinje cell firing alterations and the emergence of 160-Hz oscillation in the cerebellar cortex of $PV^{-/-}$ mice. This oscillation presents electrophysiological and pharmacological properties similar to those observed in $CB^{-/-}$ mice (Cheron *et al.*, 2004). Despite the similar electrophysiological phenotype of the two mutants, knocking-out of both genes results in the emergence of

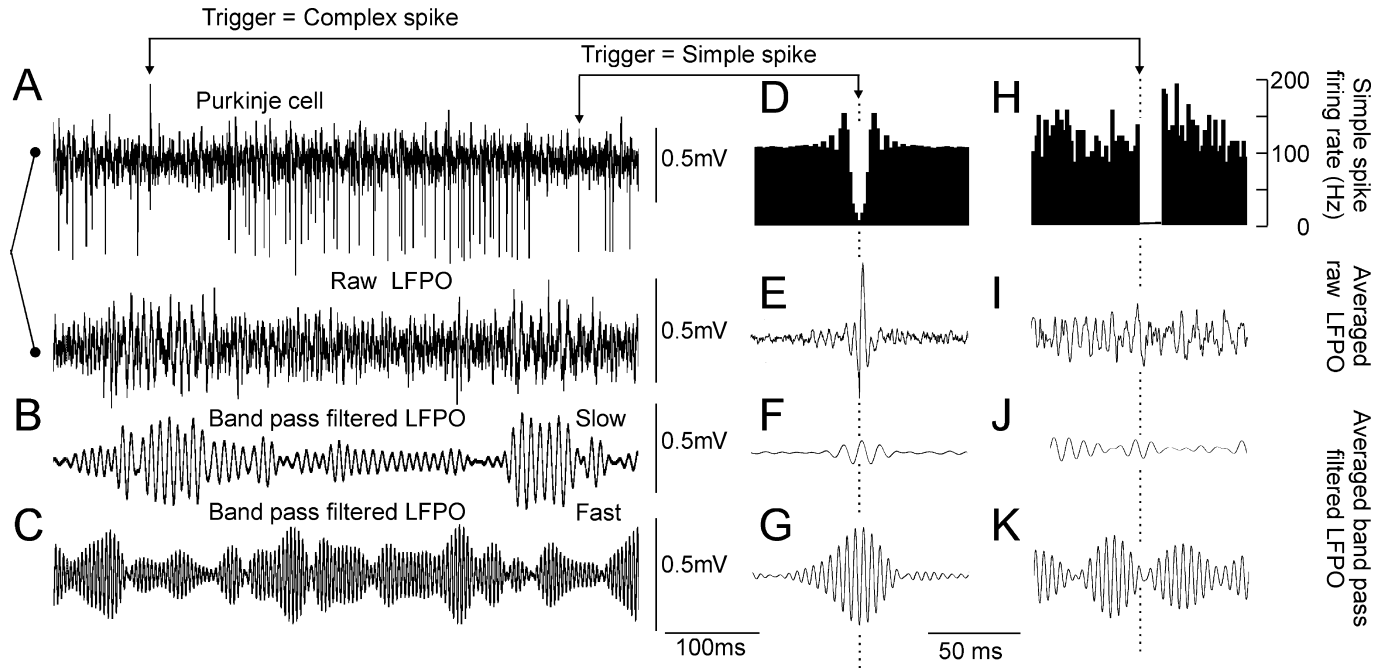


FIG. 7. Complex and simple spikes of rhythmic Purkinje cells are phase-locked to one of the frequencies of the dual-frequency local field potential oscillation (LFPO). (A) Simultaneous recording of dual-frequency LFPO and Purkinje cell along the parallel fiber axis in a mouse lacking calbindin and parvalbumin. Note the increment of interspike interval during the lowest frequency spindles. (B) Band-pass filtering between 104 and 124 Hz of the LFPO. (C) Band-pass filtering between 275 and 295 Hz of the LFPO. (D) Simple spike autocorrelogram of the Purkinje cell. Note the rhythmicity presented as small symmetrical side peaks (approx. 3). (E) Averaging of LFPO triggered by the simple spike of the Purkinje cell. Note the presence of a fast oscillation before and after the simple spike, phase-locked to the negative wave of the LFPO. (F and G) Averaging of band-pass-filtered signal as illustrated in B and C triggered by the simple spike of the Purkinje cell. Note how simple spikes are phase-locked to the rapid frequency of the dual-frequency LFPO. (H) Simple spike cross-correlogram triggered by complex spikes. (I) Averaging of LFPO triggered by the depolarization of the complex spike. Note the presence of a fast oscillation before the complex spike, phase-locked to the ascending wave of the rapid frequency. (J and K) Averaging of band-pass-filtered signal illustrated in B and C triggered by the complex spike.

dual-frequency (around 110 and 240 Hz) oscillations. This is the first report of dual-frequency oscillation above 100 Hz in the cerebellum. In other parts of the mammalian brain, high-frequency oscillations that occur at different frequencies have already been described in hippocampal (Bragin *et al.*, 1999; Csicsvari *et al.*, 1999), entorhinal (Bragin *et al.*, 2002) and somatosensory (Jones & Barth, 2002) cortex.

As with any other neuronal firing, Purkinje cell firing largely depends on intracellular Ca^{2+} homeostasis (Berridge, 1998). For example, intracellular $[\text{Ca}^{2+}]$ changes during climbing fiber activation are crucial in this regulatory process (Llinás & Sugimori, 1980; Ito, 1989; Kano *et al.*, 1992). In a slice preparation, Chang *et al.* (1993) suggested a role of intracellular Ca^{2+} in the oscillatory activity of Purkinje cells. Experimental and theoretical studies have demonstrated that neuronal rhythms of various time scales are associated with the regulation of ionic conductances that largely depend on Ca^{2+} homeostasis (Llinás, 1988; Meyer & Stryer, 1988). A major function of Ca^{2+} -binding proteins is to modulate the amplitude and kinetics of $[\text{Ca}^{2+}]$ transients. The absence of CB results in alterations in Purkinje cell firing, including decreased complex spike duration and subsequent pause and fast cerebellar LFPO supported by increased synchronicity and rhythmicity of simple spikes (Cheron *et al.*, 2004). The present results demonstrate that the absence of PV, a slower Ca^{2+} buffer, leads to similar alterations. Some of these are less pronounced in $\text{PV}^{-/-}$ than in $\text{CB}^{-/-}$ mice, namely alterations in simple spike rhythmicity, complex spike duration and pause. This could be related to the Ca^{2+} -binding properties of both buffers. Indeed, CB presents binding sites with at least two distinct binding kinetics (Nagerl *et al.*, 2000), i.e. sites with fast and sites with intermediate on-rates for Ca^{2+} binding, while both binding sites of PV are slow. One may envisage that the

intermediate sites of CB could, in part, functionally replace PV. Conversely, the slow binding sites of PV cannot replace the function of the fast sites of CB. This could explain the increased alterations observed in $\text{CB}^{-/-}$ in comparison with $\text{PV}^{-/-}$ mice. However, the present results cannot determine whether the differences in electrophysiological alterations between $\text{PV}^{-/-}$ and $\text{CB}^{-/-}$ mice are solely related to differences in the Ca^{2+} -binding kinetics of CB and PV as PV is additionally expressed in basket and stellate cells. This might affect Purkinje cell properties indirectly via a network mechanism. Such an effect has been demonstrated in mice lacking CR, a protein that in the cerebellum is almost selectively expressed in granule cells (Schiffmann *et al.*, 1999; Bearzatto *et al.*, 2004). In $\text{CR}^{-/-}$ mice, the alterations in complex and simple spikes were the same as those in $\text{PV}^{-/-}$ and $\text{CB}^{-/-}$ mice. These alterations in $\text{CR}^{-/-}$ mice are probably due to increased activation of Purkinje, stellate and basket cells, given the granule cell hyperexcitability in $\text{CR}^{-/-}$ mice (Gall *et al.*, 2003) and the absence of CR expression in WT Purkinje cells and molecular interneurons. In $\text{PV}^{-/-}$ mice, the absence of a Ca^{2+} buffer in molecular layer interneurons and Purkinje cells leads to alterations in pre-synaptic Ca^{2+} signaling (Collin *et al.*, 2005) and possibly to hyperexcitability (Gall *et al.*, 2003) of both cell types thereby producing a similar pattern of Purkinje cell complex spike and pause duration. We ruled out the possibility that the mechanism leading to the paradoxical CR immunoreactivity in Purkinje cells of $\text{CR}^{-/-}$ mice (Schiffmann *et al.*, 1999) was involved in Purkinje cell firing alteration in $\text{PV}^{-/-}$ mice. Further experiments, such as Purkinje cell-specific PV gene rescuing (knock-in), would be required to determine whether the differences in the phenotype severity between $\text{PV}^{-/-}$ and $\text{CB}^{-/-}$ mice are strictly related to differences in Ca^{2+} -binding kinetics or to the

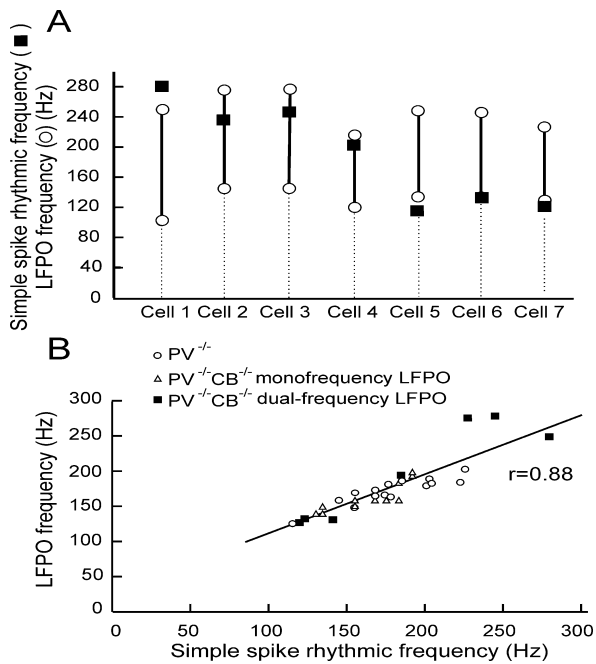


FIG. 8. Local field potential oscillation (LFPO) frequencies are very similar to simultaneously recorded Purkinje cell rhythmic frequencies. (A) Frequencies of seven dual-frequency LFPO episodes (○) and seven simultaneously recorded rhythmic Purkinje cells (■) in two mice lacking calbindin and parvalbumin (PV^{-/-}CB^{-/-}). The rhythmic frequency of each Purkinje cell is close to one of the two peak frequencies of the LFPO. (B) Plotted values of simple spike rhythmicity plotted vs. simultaneously recorded frequency of LFPO episodes in rhythmic Purkinje cells [15 mice lacking parvalbumin (PV^{-/-}), 11 PV^{-/-}CB^{-/-} mice with one-frequency oscillations and seven PV^{-/-}CB^{-/-} mice with dual-frequency oscillations].

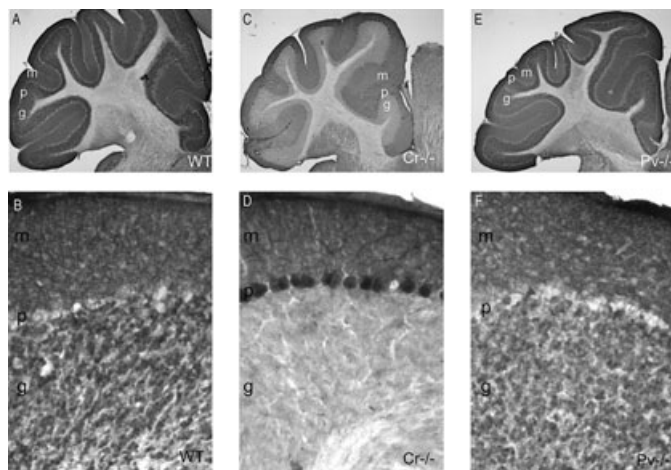


FIG. 9. Immunohistochemistry using a rabbit anti-calretinin polyclonal antibody on parasagittal sections. (A and B) Calretinin immunoreactivity in a wild-type (WT) mouse is observed in cerebellar granule cells and parallel fibers in the molecular layer (m), p, Purkinje cell layer; g, granular layer. (C and D) In mice lacking calretinin (CR^{-/-}), apparent calretinin immunoreactivity is detected in Purkinje cell bodies, dendritic trees and axons. (E and F) In mice lacking parvalbumin (PV^{-/-}), as in WT mice, the calretinin immunoreactivity is restricted to granule cells and associated parallel fibers.

additional presence of PV in basket and stellate cells in WT mice. The study of double mutants offers insights into this question. PV^{-/-}CB^{-/-} mice present a major decrement of complex spike duration and pause, with no additional increment of simple spike firing rate or rhythmicity

when compared with single mutants. This suggests that the absence of PV in the molecular interneuron may enhance complex spike alterations observed in the double mutants.

The rhythmic firing pattern of Purkinje cells that is normally absent in WT mice (Goossens *et al.*, 2001; Cheron *et al.*, 2004) leads to the emergence of ~160-Hz oscillation in PV^{-/-}, CB^{-/-} and PV^{-/-}CB^{-/-} mice. The common physiological properties of this 160-Hz LFPO include: (1) phase-locking to rhythmic Purkinje cells; (2) synchronization along the parallel fiber axis and (3) reversible inhibition by blockers of *N*-methyl-D-aspartate receptors, GABA_A receptors and gap junctions. What could be the mechanism by which deletion of a Ca²⁺-binding protein in Purkinje cells leads to the emergence of fast cerebellar oscillation? The present results demonstrate that the synchronization of rhythmic Purkinje cells is central in this process. Given the inhibitory action of gabazine and carbenoxolone on LFPO, the densely gap junction-connected interneuron network is probably involved in the maintenance of such a firing mode. This inhibitory network plays a key role in synaptic integration and precise timing of Purkinje cell spikes, enabling them to act as coincidence detectors of parallel fiber input (Mittmann *et al.*, 2005). The firing behavior of interneurons during fast LFPO remains to be studied but, to our knowledge, spontaneous activity of cerebellar interneurons in alert normal animals has never been described, as these neurons are difficult to consistently identify. Studies of different Ca²⁺-binding knockout mice demonstrate that both intrinsic and extrinsic factors may induce increased Purkinje cell rhythmicity. The intrinsic factors are demonstrated by the Purkinje cell specificity of CB, suggesting that precise control of Ca²⁺ transients in Purkinje cells (Airaksinen *et al.*, 1997) is required to control the rhythmicity of their firing. An extrinsic mechanism (network) must be involved in CR^{-/-} mice as CR is not expressed in Purkinje cells. In these mice, increased excitation of Purkinje cells by parallel fibers leads to increased firing rate and rhythmicity of Purkinje cells, facilitating the emergence of their synchronization on the same rhythmic firing pattern. Thus, it appears that fast cerebellar LFPO may result from different conditions leading to Purkinje cell rhythmicity, either through intrinsic regulation of firing or through an increase of excitatory input. In CB^{-/-}CR^{-/-} mice, where CR-depleted granule cells overexcite CB-deficient Purkinje cells, LFPO is similar to that in the single mutant, although stronger and more constant (Cheron *et al.*, 2004). In contrast, PV^{-/-}CB^{-/-} mice, where Purkinje cell Ca²⁺-buffering capacity is decreased more than in single mutants, show dual-frequency LFPO. The fact that Purkinje cells are phase-locked with one of the two frequencies rules out the possibility that both frequencies would simply be harmonics of one common rhythm and that the same Purkinje cells would sustain dual-frequency oscillation. Thus, it is the rhythmic and synchronous firing of different Purkinje cell populations firing at different rhythmic frequencies in PV^{-/-}CB^{-/-} mice outlines the increased tendency of Purkinje cells lacking Ca²⁺ buffers to fire in a rhythmic and synchronous mode, regardless of the calcium-binding properties of the buffer. During the recording, the two frequencies could merge into a mono-frequency LFPO around 200 Hz and split again to dual-frequency oscillation, indicating a dynamic process.

This dual mode may be facilitated by the heterogeneity of the Purkinje cell population previously revealed following ischemia (Welsh *et al.*, 2002). The intrinsic nature of the Purkinje cell bistability (Loewenstein *et al.*, 2005) may facilitate LFPO bifurcation by switching Purkinje cells between up and down states of firing. In the same line of reasoning, cutaneous stimulation was able to simultaneously evoke excitation and inhibition of different Purkinje

cell populations (Bower & Woolston, 1983; Cheron *et al.*, 2004) leading to a reciprocal firing mode resembling that recorded during dual fast oscillation.

In conclusion, the present data demonstrate that the cytosolic Ca²⁺ buffers CB D-28k and PV play a key role in the regulation of Purkinje cell firing rate and rhythmicity *in vivo*. Our results also suggest that precise Ca²⁺ transient control by these binding proteins is required to maintain the spontaneous firing pattern of the Purkinje cells arrhythmic and asynchronous, which is necessary for normal cerebellar functioning.

Acknowledgements

L.S. and B.B. were supported by a grant of 'Fondation Erasme' and by FRIA (Belgium), respectively. L.S. and M.D. are presently funded by the Belgian National Fund for Scientific Research (FNRS). The expert assistance of L. Cuvelier and M.P. Dufief in immunocytochemistry and electrophysiology is acknowledged. The authors specially thank Dr R. Leach for his comment on the manuscript. This work was supported by the FNRS, FMRE (Belgium), Van Buuren Foundation (Belgium), research funds of ULB and UMH, Belgium, Action de Recherche Concertée (ARC) and the Swiss National Science Foundation grants 3100-063448.00/1 and 3100A0-100400/1 (to B.S.).

Abbreviations

CB, calbindin; CB^{-/-}, mice lacking calbindin; CR, calretinin; CR^{-/-}, mice lacking calretinin; LFPO, local field potential oscillation; PV, parvalbumin; PV^{-/-}, mice lacking parvalbumin; PV^{-/-}CB^{-/-}, mice lacking calbindin and parvalbumin; WT, wild-type.

References

- Airaksinen, M.S., Eilers, J., Garaschuk, O., Thoenen, H., Konnerth, A. & Meyer, M. (1997) Ataxia and altered dendritic calcium signaling in mice carrying a targeted null mutation of the calbindin D28k gene. *Proc. Natl Acad. Sci. U.S.A.*, **94**, 1488–1493.
- Andressen, C., Blumcke, I. & Celio, M.R. (1993) Calcium-binding proteins: selective markers of nerve cells. *Cell Tissue Res.*, **271**, 181–208.
- Barski, J.J., Hartmann, J., Rose, C.R., Hoebeek, F., Morl, K., Noll-Hussong, M., De Zeeuw, C.I., Konnerth, A. & Meyer, M. (2003) Calbindin in cerebellar Purkinje cells is a critical determinant of the precision of motor coordination. *J. Neurosci.*, **23**, 3469–3477.
- Bearzatto, B., Servais, L., Gall, G., Roussel, C., Baba-Aissa, F., de Kerchove d'Exaerde, A., Schurmans, S., Cheron, G. & Schiffmann, S.N. (2004) Selective expression of calretinin into cerebellar granule cells is essential for granule cell excitability, Purkinje cells firing, and motor coordination. *Soc. Neurosci. Abstr.* 827.9.
- Berridge, M.J. (1998) Neuronal calcium signaling. *Neuron*, **21**, 13–26.
- Bower, J.M. & Woolston, D.C. (1983) Congruence of spatial organization of tactile projections to granule cell and Purkinje cell layers of cerebellar hemispheres of the albino rat: vertical organization of cerebellar cortex. *J. Neurophysiol.*, **49**, 745–766.
- Bragin, A., Engel, J. Jr, Wilson, C.L., Fried, I. & Mathern, G.W. (1999) Hippocampal and entorhinal cortex high-frequency oscillations (100–500 Hz) in human epileptic brain and in kainic acid-treated rats with chronic seizures. *Epilepsia*, **40**, 127–137.
- Bragin, A., Wilson, C.L., Staba, R.J., Reddick, M., Fried, I. & Engel, J. Jr (2002) Interictal high-frequency oscillations (80–500 Hz) in the human epileptic brain: entorhinal cortex. *Ann. Neurol.*, **52**, 407–415.
- Celio, M.R. (1990) Calbindin D-28k and parvalbumin in the rat nervous system. *Neuroscience*, **35**, 375–475.
- Chang, W., Strahlendorf, J.C. & Strahlendorf, H.K. (1993) Ionic contributions to the oscillatory firing activity of rat Purkinje cells in vitro. *Brain Res.*, **614**, 335–341.
- Cheron, G., Gall, D., Servais, L., Dan, B., Maex, R. & Schiffmann, S.N. (2004) Inactivation of calcium-binding protein genes induces 160 Hz oscillations in the cerebellar cortex of alert mice. *J. Neurosci.*, **24**, 434–441.
- Collin, T., Chat, M., Lucas, M.G., Moreno, H., Tacay, P., Schwaller, B., Marty, A. & Llano, I. (2005) Developmental changes in parvalbumin regulate axonal Ca²⁺ signalling. *J. Neurosci.*, **25**, 96–107.
- Csicsvari, J., Hirase, H., Czurko, A., Mamiya, A. & Buzsáki, G. (1999) Fast network oscillations in the hippocampal CA1 region of the behaving rat. *J. Neurosci.*, **19**, 1–4.
- Eckhorn, R. & Thomas, U. (1993) A new method for the insertion of multiple microprobes into neural and muscular tissue, including fiber electrodes, fine wires, needles and microsensors. *J. Neurosci. Meth.*, **49**, 175–179.
- Fierro, L., DiPolo, R. & Llano, I. (1998) Intracellular calcium clearance in Purkinje cell somata from rat cerebellar slices. *J. Physiol. (Lond.)*, **510**, 499–512.
- Fortin, M., Marchand, R. & Parent, A. (1998) Calcium-binding proteins in primate cerebellum. *Neurosci. Res.*, **30**, 155–168.
- Gall, D., Roussel, C., Susa, I., D'Angelo, E., Rossi, P., Bearzatto, B., Galas, M.C., Blum, D., Schurmans, S. & Schiffmann, S.N. (2003) Altered neuronal excitability in cerebellar granule cells of mice lacking calretinin. *J. Neurosci.*, **15**, 9320–9327.
- Goossens, J., Daniel, H., Rancillac, A., van der Steen, J., Oberdick, J., Crepel, F., De Zeeuw, C.I. & Frens, M.A. (2001) Expression of protein kinase C inhibitor blocks cerebellar long-term depression without affecting Purkinje cell excitability in alert mice. *J. Neurosci.*, **21**, 5813–5823.
- Ito, M. (1989) Long-term depression. *Annu. Rev. Neurosci.*, **12**, 85–102.
- Jones, M.S. & Barth, D.S. (2002) Effects of bicuculline methiodide on fast (>200 Hz) electrical oscillations in rat somatosensory cortex. *J. Neurophysiol.*, **88**, 1016–1025.
- Kano, M., Rexhausen, U., Dreessen, J. & Konnerth, A. (1992) Synaptic excitation produces a long-lasting rebound potentiation of inhibitory synaptic signals in cerebellar Purkinje cells. *Nature*, **356**, 601–604.
- Lee, S.H., Schwaller, B. & Neher, E. (2000) Kinetics of Ca²⁺ binding to parvalbumin in bovine chromaffin cells: implications for [Ca²⁺] transients of neuronal dendrites. *J. Physiol. (Lond.)*, **525**, 419–432.
- Llinás, R. (1988) The intrinsic electrophysiological properties of mammalian neurons: insights into central nervous system function. *Science*, **242**, 1654–1664.
- Llinás, R. & Sugimori, M. (1980) Electrophysiological properties of in vitro Purkinje cell dendrites in mammalian cerebellar slices. *J. Physiol. (Lond.)*, **305**, 197–213.
- Loewenstein, Y., Mahon, S., Chadderton, P., Kitamura, K., Sompolinsky, H., Yarom, Y. & Hausser, M. (2005) Bistability of cerebellar Purkinje cells modulated by sensory stimulation. *Nat. Neurosci.*, **8**, 202–211.
- Meyer, T. & Stryer, L. (1988) Molecular model for receptor-stimulated calcium spiking. *Proc. Natl Acad. Sci. U.S.A.*, **85**, 5051–5055.
- Mittmann, W., Koch, U. & Hausser, M. (2005) Feed-forward inhibition shapes the spike output of cerebellar Purkinje cells. *J. Physiol.*, **563**, 369–378.
- Nagerl, U.V., Novo, D., Mody, I. & Vergara, J.L. (2000) Binding kinetics of calbindin-D(28k) determined by flash photolysis of caged Ca(2+). *Biophys. J.*, **79**, 3009–3018.
- Schiffmann, S.N., Cheron, G., Lohof, A., d'Alcantara, P., Meyer, M., Parnantier, M. & Schurmans, S. (1999) Impaired motor coordination and Purkinje cell excitability in mice lacking calretinin. *Proc. Natl Acad. Sci. U.S.A.*, **96**, 5257–5262.
- Schmidt, H., Brown, E.B., Schwaller, B. & Eilers, J. (2003) Diffusional mobility of parvalbumin in spiny dendrites of cerebellar Purkinje neurons quantified by fluorescence recovery after photobleaching. *Biophys. J.*, **84**, 2599–2608.
- Schwaller, B., Dick, J., Dhoot, G., Carroll, S., Vrbova, G., Nicotera, P., Pette, D., Wyss, A., Bluethmann, H., Hunziker, W. & Celio, M.R. (1999) Prolonged contraction-relaxation cycle of fast-twitch muscles in parvalbumin knockout mice. *Am. J. Physiol.*, **276**, 395–403.
- Schwaller, B., Meyer, M. & Schiffmann, S.N. (2002) 'New' functions for 'old' proteins: the role of the calcium-binding proteins calbindin D-28k, calretinin and parvalbumin, in cerebellar physiology. Studies with knockout mice. *Cerebellum*, **1**, 241–258.
- Servais, L. & Cheron, G. (2005) Purkinje cell rhythmicity and synchronicity during modulation of fast cerebellar oscillation. *Neuroscience*, in press. [doi: 10.1016/j.neuroscience.2005.06.001]
- Steriade, M., Amzica, F., Neckelmann, D. & Timofeev, I. (1998) Spike-wave complexes and fast components of cortically generated seizures. II. Extra- and intracellular patterns. *J. Neurophysiol.*, **80**, 1456–1479.
- Sugihara, I., Lang, E.J. & Llinás, R. (1995) Serotonin modulation of inferior olivary oscillations and synchronicity: a multiple-electrode study in the rat cerebellum. *Eur. J. Neurosci.*, **7**, 521–534.
- Vecellio, M., Schwaller, B., Meyer, M., Hunziker, W. & Celio, M.R. (2000) Alterations in Purkinje cell spines of calbindin D-28 k and parvalbumin knockout mice. *Eur. J. Neurosci.*, **12**, 945–954.
- Welsh, J.P., Yuen, G., Placantonakis, D.G., Vu, T.Q., Haiss, F., O'Hearn, E., Molliver, M.E. & Aicher, S.A. (2002) Why do Purkinje cells die so easily after global brain ischemia? Aldolase C, EAAT4, and the cerebellar contribution to posthypoxic myoclonus. *Adv. Neurol.*, **89**, 331–359.